Rare Metal Materials and Engineering
Volume 50, Issue 2, February 2021
Available online at www.rmme.ac.cn

Science Press

Cite this article as: Rare Metal Materials and Engineering, 2021, 50(2): 0396-0407.

ARTICLE

Material Removal Mechanism of Single Crystal γ-TiAl Alloy by Double Abrasive Micro Cutting

Li Junye, Xie Hongcai, Zhang Xinming, Zhao Weihong, Shi Guangfeng, Xu Chengyu

Ministry of Education Key Laboratory for Cross-Scale Micro and Nano Manufacturing, Changchun University of Science and Technology, Changchun 130022, China

Abstract: In order to analyze the material removal mechanism of single crystal γ-TiAl alloy in grinding, the molecular dynamics model of Ti-Al alloy ground by two abrasive grains was established. The influence of lateral and longitudinal spacing of the diamond abrasive on the material removal mechanism of the single crystal γ-TiAl alloy was revealed. The results show that the micro cutting process of single crystal γ-TiAl alloy is accompanied by the change of temperature, potential energy, dislocation, as well as lattice phase transition. Cutting force, cutting temperature, potential energy and removal efficiency increase with the increase of lateral spacing, but are less affected by longitudinal spacing. The number of lattice phase transition atoms increases with the increase of lateral spacing and decreases with the increase of longitudinal spacing. With the increase of lateral and longitudinal spacing, the number of dislocations, total length of dislocations, and density of dislocations increase accordingly.

Key words: single crystal γ-TiAl alloy; material removal mechanism; molecular dynamics

Abrasive flow machining (AFM), as one kind of precision finishing technology, can realize the finishing processing of special channel surface and small size parts. It can also improve precision of the workpiece surface and deal with complex shape parts which traditional processing methods cannot achieve. The application of AFM is increasingly wide[1,2], and more scholars research on this technique. Petare[3] et al conducted experiments to study the impact of abrasive flow precision machining on wear characteristics, surface finish and microstructure of spur bevel gear (SBG). Zhang[4] et al discussed the research on the precision machining of the constrained abrasive flow on the surface of complex titanium alloy through numerical and experimental studies, and found that triangular restraint plate can greatly improve the polishing efficiency and quality.

However, the cutting effect occurs in the partial area of the workpiece surface, which is under micro scale. Molecular dynamics is a powerful tool to overcome this difficulty. So molecular dynamics simulation for studying micro cutting process has attracted great attention. Li[5] et al used molecular dynamics simulation to study the micro cutting of single crystal copper by SiC abrasive at different cutting angles, and found that a small cutting angle is beneficial to improve the surface quality and reduce internal defects. Lai[6] et al studied the surface morphology, cutting force and subsurface deformation of monocrystal germanium in the process of partially overlapping nanometer cutting with different feedstock, and found that the side-flow material stacked at the edge of the cutting edge is the decisive factor of processing parameters affecting the surface morphology. Alhafez[7] et al studied the effects of different surface orientations and cutting directions on the nanocrystalline iron cutting process. Zhu[8] et al studied nanometer cutting single crystal nickel. Through the analysis of atomic displacement and change of cutting force, it was found that the generation of complex stacking fault is the main cause of cutting force fluctuations. He[9] et al studied the subsurface damage mechanism of monocrystalline silicon at different grinding speeds and found that increasing the

Received date: February 20, 2020
Foundation item: National Natural Science Foundation of China (51206011, U1937201); Science and Technology Development Program of Jilin Province (20200301040RQ); Project of Education Department of Jilin Province (JJKH20190541KJ); Science and Technology Program of Changchun City (18DY017)
Corresponding author: Zhang Xinming, Ph. D., Professor, Changchun University of Science and Technology, Changchun 130022, P. R. China, E-mail: fstving@163.com

grinding speed at low speeds can reduce the damage thickness of subsurface. Zhu[10] et al used molecular dynamics simulation to study the titanium micro cutting process and found that the cutting process and the formation of the processed surface are caused by the release of lattice energy and the continuous expansion of dislocations.

As a new kind of metal compound structural material, γ-TiAl alloy has many outstanding characteristics: low density, high specific strength, strong creep resistance and oxidation resistance, and high strength and stiffness at high temperatures. It is extremely competitive in aerospace and other fields. At present, there are few studies on single crystal γ-TiAl alloy cutting at the micro scale. Feng[11] et al studied the effect of different cutting speeds and cutting depths on the process of micro-cutting γ-TiAl alloy. Li[12] et al studied the influence of cutting crystal orientation on the process of micro cutting single crystal γ-TiAl alloy. However, only one kind of abrasive particle was used in the study, which is different from the actual machining process of abrasive particle flow. At present, some researchers have studied the material process of multi-abrasive micro-cutting workpiece. Li[5,13] et al established molecular dynamics simulation of single crystal copper in double abrasive nanometer cutting and studied the influence of cutting angle on the nanometer cutting process. Later, molecular dynamics simulation was carried out for the process of polishing polycrystalline materials (copper, aluminum and iron) with double abrasive particles, and the effects of cutting depth and abrasive type on the cutting force, energy, friction coefficient and surface morphology of the three polycrystalline materials were analyzed. Zhou[14] et al used molecular dynamics method to simulate double abrasive polishing single crystal SiC, and studied the effects of cutting depth and abrasive spacing on phase transition, subsurface layer thickness, surface quality, material removal efficiency and friction characteristics. In order to achieve real processing conditions and improve cutting efficiency in micro cutting single crystal γ-TiAl alloy process, two diamond abrasive micro-cutting workpieces were set up in this work, and the relative lateral and longitudinal spacing of two abrasive particles were measured to study the effect of transverse and longitudinal spacing on the material removal mechanism of abrasive particles micro cutting. It can provide theoretical basis and technical support for practical abrasive flow machining.

1 Model Establishment and Selection of Potential Function

1.1 Model establishment

There is a slight difference between the crystal structure of the γ-TiAl alloy and the ordinary face centered cubic (fcc) crystal structure. γ-TiAl alloy has the face-centered tetragonal (fct) with $L1_0$ structure. The lattice constants are a=b=0.4001 nm and c=0.4181 nm. The first step of molecular dynamics numerical analysis is to construct the molecular dynamics simulation model of abrasive micro cutting. The established molecular dynamics model of diamond abrasive micro cutting single crystal γ-TiAl alloy is shown in Fig.1. The x, y and z directions correspond to [100], [010] and [001] directions, respectively. Single crystal γ-TiAl alloy was selected as the cutting workpiece. The model size is 10 nm×16 nm×8 nm. The diamond abrasive grains with lattice constant of 0.357 nm were selected as the grinding grains, and the abrasive radius is 1.5 nm. The number of atoms in the cutting workpiece and the grinding particle is 80 000 and 4965, respectively. In order to improve cutting efficiency and achieve more realistic AFM conditions, the molecular dynamics model established in this work adopts two diamond abrasive particles for cutting action, and the relative position arrangement of the fixed double abrasive particles is shown in Fig.2. In order to investigate the effect of lateral (x direction) spacing and longitudinal (y direction) spacing on abrasive removal materials, the lateral spacing of the two diamond abrasive particles was set as 1, 1.5, 2 and 2.5 nm, the longitudinal spacing was set as 2, 2.5 and 3 nm, and the cutting depth was set as 1 nm. To save calculation efficiency, the cutting speed was set as 200 m/s.

In the established molecular dynamics model of micro cutting single crystal γ-TiAl alloys for diamond abrasive particles, both the workpiece model and the abrasive particle model were modeled by LAMMPS. Firstly, a cuboid simulation box (16 nm×24 nm×15 nm) was created, the simulated atom types (Ti, Al, C) were defined, the workpiece area and grinding particle area were set in the simulation box, the lattice structure of the workpiece and grinding particle was

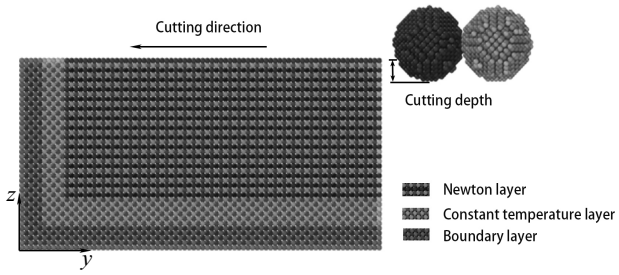

Fig.1 Molecular dynamics model of micro cutting single crystal γ-TiAl alloy with diamond grains

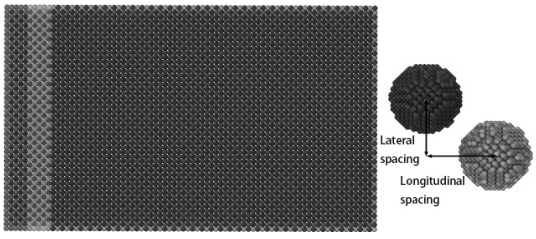

Fig.2 Fixed relative position arrangement of the double grinding grains

determined, the workpiece atom and grinding particle atom were created, and the model force field parameters and simulation parameters were set. Similar to the traditional molecular dynamics simulation of abrasive flow processing, the workpiece model was divided into three regions: the boundary layer, the thermostatic layer and the Newton layer (processing region). In order to fix the workpiece, the atoms of the boundary layer remained stationary. The thermostatic layer is used to transfer heat and ensure the heat exchange of the system. Newton layers are used to simulate the motion of atoms. After the whole model was built, the initial temperature was set at 293 K, but the system was at an unstable state. To make the system reach equilibrium state, the Nose-Hoover hot bath method was used to relax the system. Since the hardness of the diamond is far greater than that of the workpiece, without considering the internal force, the diamond abrasive particles were set as rigid bodies and placed on the upper right of the workpiece. After relaxation, they moved along the $-y$ direction at the speed of 200 m/s for cutting.

1.2 Selection of the potential energy function

The interaction behavior between atoms is described by the potential function. In the process of numerical analysis of molecular dynamics, the interactions between Ti-Al, Ti-C and Al-C need to be considered because diamond abrasive grains were set as rigid bodies.

Embedded atomic method (EAM) can accurately describe the interaction between metal atoms. It is the most widely used interatomic potential of metals and alloys and can effectively describe the interaction between metal atoms. In this study, the EAM potential was selected to describe the interaction potential between Ti-Al[15], and the atomic energy is expressed as:

$$E = \sum_i F_i(\rho_i) + \frac{1}{2}\sum_{j\neq i} \Phi_{ij}(r_{ij}) \quad (1)$$

where F_i is the embedded energy function of the density of the atom i, ρ_i is the electron cloud density of other atoms, Φ_{ij} is the potential interaction function between the i atom and the j atom, and r_{ij} is the distance between the i atom and the j atom.

Morse potential function is a typical potential model based on the diatomic theory, which has a good approximation to the fine structure of atomic vibration. In this study, Morse potential was used to describe the interaction between Ti-C and Al-C[16], and the expression is as follows:

$$E = D[e^{-2\alpha(r_{ij}-r)} - 2e^{-\alpha(r_{ij}-r)}] \quad (2)$$

where D is the binding energy, α is the elastic modulus coefficient, r_{ij} is the distance between the i atom and the j atom, and r is the atomic spacing at equilibrium.

In addition, in the process of molecular dynamics numerical analysis, Ackland-Jones analysis was used to identify the crystal structure in the workpiece[17], and dislocation extraction algorithm was used to identify the dislocation defects in the crystal[18].

2 Analysis and Discussion

2.1 Removal mechanism analysis of abrasive micro cutting materials

2.1.1 Analysis of material removal during micro cutting

In the absence of external force, the atoms of the workpiece are arranged regularly and orderly in space. In the process of micro cutting, the workpiece is affected by the cutting force of abrasive particles, the surface of workpiece materials extrudes and deforms, and the atoms of workpiece are displaced, resulting in a large number of workpiece materials piled up in front of abrasive particles. In order to study the removal mechanism of workpiece materials in abrasive flow machining, the lateral spacing x is set as 2.5 nm, the longitudinal spacing y is set as 3 nm, the cutting depth is set as 1 nm, and the cutting speed is set as 200 m/s. Fig.3 shows the surface profile of the workpieces with the cutting distance of 3, 6, 9 and 12 nm in the process of abrasive micro cutting, in which the wireframe along the edge of the mesh surface is rendered. As the cutting distance increases, the workpiece atoms move along the cutting direction with the abrasive particles, and the number of workpiece atoms in contact with the abrasive particles increases. In the cutting area, the workpiece atoms pile up at the front and both sides of the abrasive particles, and the atomic height of the workpiece piled up in the z direction increases, finally achieving the purpose of material removal. Fig.4 shows the surface morphologies of the workpiece when the cutting distance is 3, 6, 9 and 12 nm during the micro cutting process of the abrasive particles, in which the workpiece atom is colored according to its height along the z-axis. In the process of micro cutting, the workpiece atoms are squeezed by the abrasive atoms to generate displacement, and a large number of atoms pile up in front of the abrasive particles to form chips. At the same time, there are protrusions on both sides of the grooves generated by the cutting action of the abrasive particles, and the side flow forms. As the cutting distance increases, more and more workpiece atoms accumulate in front of the abrasive particles, some of which remove in the form of chips as the abrasive particles move, and some of which remain on both sides of the groove to form the machined surface in the form of side flow. When the cutting distance is 3 nm, the first abrasive particle cuts into the workpiece completely, and the second abrasive particle begins to contact the workpiece. When the cutting distance is 6 nm, the first and even the second abrasive particle cut into the workpiece completely, and part of the atoms gradually accumulate at the intersection of the two abrasive particle cutting trajectories. Therefore, the micro cutting process of abrasive particles can be divided into two stages. In the first stage, when the cutting distance is no more than 3 nm, only one abrasive particle can cut the workpiece. In the second stage, when the cutting distance is more than 3 nm, indicating that the cutting distance exceeds the longitudinal distance

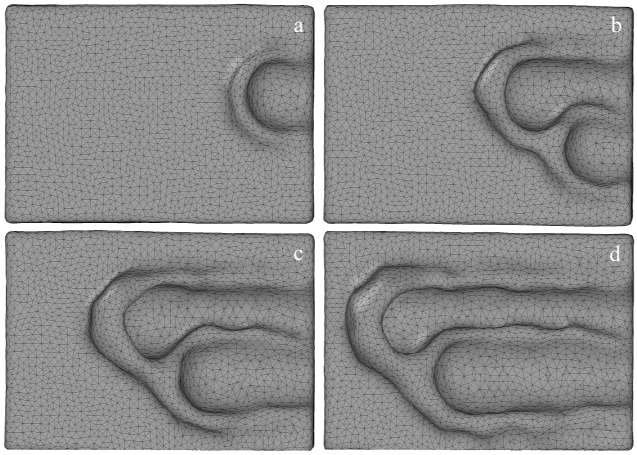

Fig.3 Surface profiles of workpiece during micro cutting with cutting distance of 3 nm (a), 6 nm (b), 9 nm (c) and 12 nm (d)

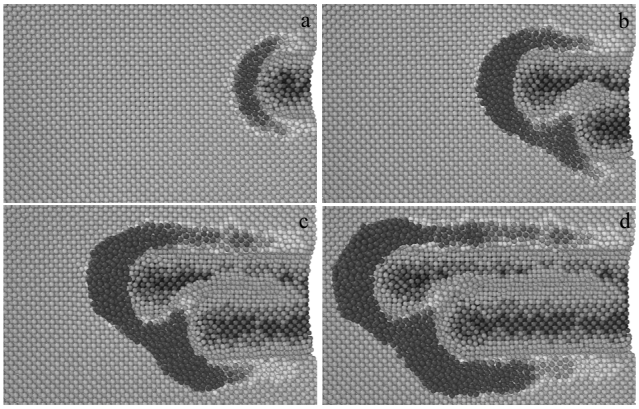

Fig.4 Surface morphologies of workpiece during micro cutting with cutting distance of 3 nm (a), 6 nm (b), 9 nm (c) and 12 nm (d)

between the two grinding grains, the two grinding grains act on the workpiece simultaneously. When the cutting distance is more than 3 nm, the temperature, energy, cutting force, lattice structure and dislocation of workpiece change significantly.

2.1.2 Analysis of cutting force change during micro cutting

The cutting force of the abrasive atom on the workpiece atom is an important physical parameter which can indirectly reflect the removal process of the workpiece material. In the process of micro cutting, when the abrasive particles contact with the surface of the workpiece, the workpiece is squeezed by the abrasive particles. The purpose of micro cutting is achieved by breaking the chemical bonds between the atoms of the workpiece and forcing the atoms of the workpiece to produce displacement. In order to study the variation of the cutting force of diamond particles acting on the workpiece during the micro cutting process, this study made a statistical analysis of the variation of the cutting force of diamond particles acting on the workpiece in each direction during the micro cutting process (Fig.5). As the abrasive particles move along the $-y$ direction, the force F_y in the y direction is the main cutting force. In addition, F_x and F_z represent lateral and normal cutting forces, respectively. As shown in Fig.5a, when the cutting distance is no more than 3 nm, only one abrasive particle has a cutting effect on the workpiece. F_x does not increase or decrease continuously but fluctuates up and down around F_x=0 nN. Both the main cutting force F_y and the normal cutting force F_z show a tendency of increasing obviously with slight fluctuation. As the number of atoms in contact increases, the amplitude of the fluctuation increases. When the cutting distance increases to 3 nm, the second grinding particle begins to contact with the workpiece. F_x still fluctuates up and down around F_x=0 nN, but the fluctuation range becomes larger and larger. The main cutting force F_y and the normal cutting force F_z continue to increase. This is because the workpiece is cut by two abrasive particles at the same time, and the number of atoms in contact is higher. When the cutting distance increases to 6 nm, the second diamond abrasive particle cuts into the workpiece completely, and the cutting process begins to enter the stable cutting stage. F_y and F_z do not continue to increase but fluctuate up and down within a certain range. This is because the fluctuation of cutting force is closely related to lattice deformation, lattice

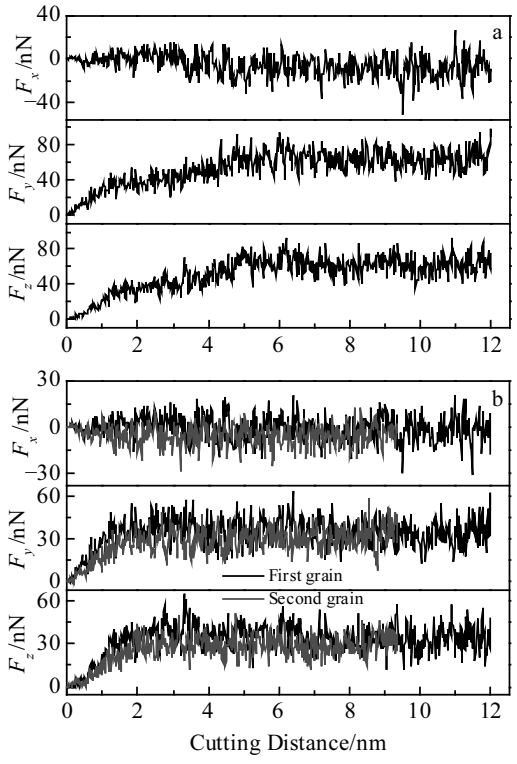

Fig.5 Variation curves of cutting forces acting on the workpiece in each direction during micro cutting: (a) total cutting force and (b) cutting forces exerted by two abrasive particles

reconstruction and the generation of amorphous structure. When the cutting force on the workpiece continues to increase and exceeds the critical value of the bonding force among the workpiece atoms, the atomic lattice of the workpiece in the cutting area is destroyed, the chemical bonds among the atoms are broken, the regular lattice structure is destroyed, and a few atoms are converted into amorphous structure. As shown in Fig.5b, when the cutting distance is 3 nm, the main cutting force and the normal cutting force of the two abrasive particles no longer keep increasing but continue to fluctuate within a certain range. The difference is that whichever the lateral cutting force, the normal cutting force, or the main cutting force of the first grinding grain, it is always greater than that of the second grinding grain cutting force.

2.1.3 Analysis of temperature and potential energy change during micro cutting

In order to study the change of the Newton layer temperature and potential energy of the workpiece in grinding, the Newton layer temperature and potential energy of the workpiece in grinding are statistically analyzed. The change of the Newton layer temperature and potential energy of the workpiece in grinding is shown in Fig.6. As shown in Fig.6a, while the cutting distance is short, Newton layer cutting zone temperature rises rapidly. This is due to the abrasive contact of the workpiece and squeeze workpiece atoms at first. Then the atomic lattice artifacts are destroyed, the original lattice structure change, chemical bonds between the atoms disconnect, forced displacement of workpiece atoms occurs, and kinetic energy increases. These conditions make the temperature of cutting zone increase. When the cutting distance is 3 nm, the second abrasive particle begins to contact the workpiece, and the first abrasive particle cuts into the workpiece completely. The temperature in the cutting area continues to rise, because more atoms in the workpiece encounter carbon atoms, generating more heat. With the increase of cutting distance, after the second abrasive particle cuts into the workpiece completely, both abrasive particles enter the stable cutting stage. The increasing temperature in the cutting area of Newton layer gradually flattens out, and the temperature keeps fluctuating around 400 K. As shown in Fig.6b, with the increase of cutting distance, the potential energy of the workpiece atom keeps increasing with slight fluctuations. This is due to the dislocation defect movement during the cutting process. From the perspective of atomic potential energy, with the continuous cutting, carbon atoms interact with the workpiece atoms, and the strain energy accumulated in the workpiece lattice exceeds the critical value of the bond. The lattice structure is destroyed, and the strain energy is released, resulting in the gradual increase of the workpiece potential energy. When the cutting distance is more than 6 nm, the potential energy of the workpiece atom increases slowly. This is because both abrasive particles cut into the workpiece completely, and the subsequent cutting process gradually tends to be stable and enters the stable cutting stage.

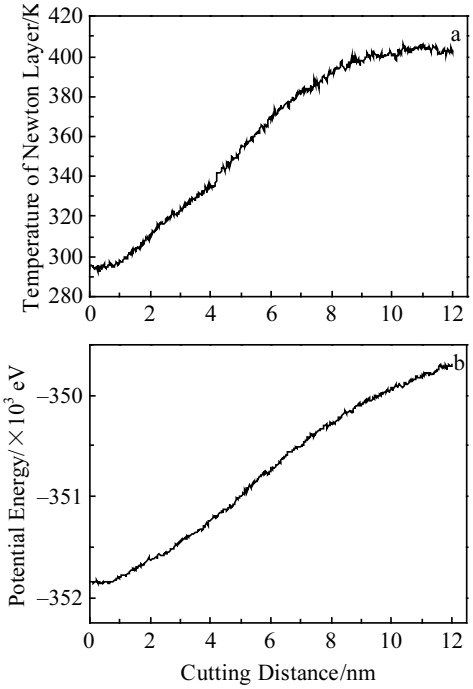

Fig.6 Newton layer temperature change (a) and potential energy change (b) of workpiece during micro cutting

2.1.4 Analysis of lattice transformation and dislocation change during micro cutting

In order to study the evolution law of various types of crystal structures, Ackland-Jones analysis method was used to identify the crystal structures in the workpiece during micro cutting, and the variation of the number of atoms in each crystal structure with the cutting distance was analyzed. Atomic lattice structure of workpiece and the quantity change during the abrasive micro cutting process are shown in Fig.7. Fig.7a shows the atomic lattice structure of the workpiece when the cutting distance is 8 nm. In order to facilitate the observation and analysis, the perfect fcc lattice is hidden from their artifacts (fcc) structure. White, red, blue, yellow atoms represent different atoms, close the six-party (hcp) structure, bcc structure and icosahedron (ico) structure, respectively. Different atoms including surface atoms and defective face-centered cubic (dfcc) structure atoms. In order to achieve the purpose of material removal, the cutting force generated by the abrasive particles destroys the original lattice structure in the cutting area of the workpiece, and the atoms of the workpiece generate displacement, which piles up on the surface of the workpiece and the front end of the abrasive particles. This process is accompanied by the generation of various lattice structures. In addition to fcc structure and the atoms, there are also hcp, bcc and ico structures in the workpiece during the micro cutting process. These structures

constantly change with the progress of cutting. The outer layer of the workpiece is identified as the atoms. In addition, the atoms are basically distributed in the processed region, and part of atomic structures transform into other lattice structures, and part of them form atomic clusters, which eventually are removed from the surface of the workpiece in the form of chips. Fig.7b shows the change curves of the number of lattice structures. Black, red, blue and pink lines represent the change in the number of atoms of dfcc, hcp, bcc and ico structures, respectively. Due to the cutting effect of the abrasive particles on the workpiece, the original arrangement state changes, and the original regular lattice structure is destroyed. Part of the arrangement of atoms becomes disordered, most of which transforms into dfcc structure, and a small number of atoms undergo phase transformation to produce other lattice structures. It can also be seen from Fig.7b that the number of hcp and bcc structures generated by phase transition is relatively large, while the number of ico structures is relatively small. As the cutting distance increases, the number of atoms in various crystal structures increases. The number of atoms reaches 2698 when the cutting distance is 12 nm. The highest number of hcp structures and bcc structures generated by fcc structure transformation is 665 and 502, respectively, which is small. The number of ico structures generated by fcc structure transformation of only 84 is the lowest. When the cutting distance is less than 3 nm, the first grinding particle does not completely cut into the workpiece, and the number of atoms in various types of structures increases gradually. The number of transitions between hcp structure and bcc structure is small and basically consistent. When the cutting distance is 3 nm, the first abrasive particle cuts into the workpiece completely, and the second abrasive particle starts to contact the workpiece. The number of atoms in various types of structures increases faster, and the variance of dfcc structure is the most obvious. When the cutting distance reaches 6 nm, the two grinding particles cut into the workpiece completely, and the increasing trend of the number of structures in the subsequent cutting process slows down and even decreases, which may be caused by the formation, expansion and annihilation of dislocation and other crystal defects.

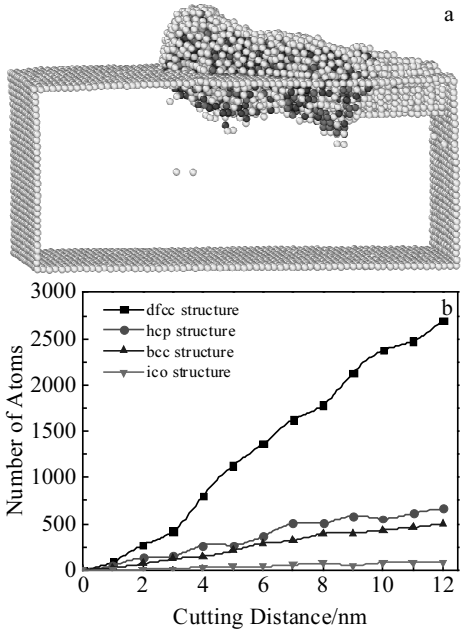

Fig.7 Atomic lattice structure of workpiece with cutting distance of 8 nm (a) and atomic quantity change curves of workpiece (b) during abrasive micro cutting

Dislocation is a configuration of partial abnormal arrangement of atoms in crystalline materials. The existence of dislocation has a very important effect on the properties of materials. In order to study the evolution of dislocation in the workpiece during micro cutting, dislocation extraction algorithm was used to identify the dislocation defects in the workpiece during micro cutting. Fig.8 shows the dislocation distribution when the cutting distance is 8 nm. In Fig.8, green and blue represent 1/6<112> Shocklley dislocation and 1/2<110> perfect dislocation, respectively. In the partially enlarged image, the Burgers vector in dark blue represents the direction of each dislocation. The Burgers vector represents the degree of lattice distortion in the dislocation region, reflecting the size and direction of local dislocation in the crystal. During the micro cutting process, the workpiece is squeezed and cut by diamond abrasive particles, the workpiece atoms in the cutting area shift, and the original lattice structure changes, resulting in dislocation in the workpiece material. As shown in Fig.8, dislocation occurs in the region with complex lattice change in the lower part of the front side of the abrasive grains, and some dislocations are interwoven with each other in a certain form. As the cutting performs, the dislocations continue to be stressed by the abrasive grains. Each segment of the dislocations slips along the direction of its Burgers vector. Some of the dislocations slip to the surface of the workpiece and disappear.

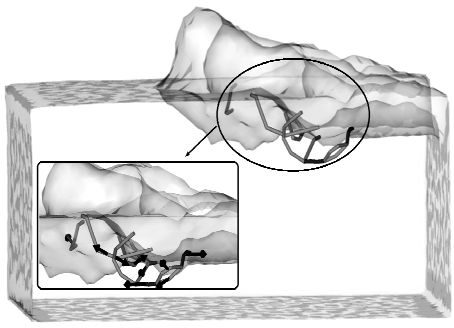

Fig.8 Dislocation distribution during micro cutting

2.2 Effect of lateral spacing on cutting process

2.2.1 Effect of lateral spacing on material removal during micro cutting

In order to study the influence of the lateral spacing of the double abrasive grains on the micro cutting process, the lateral spacing x is set as 1, 1.5, 2 and 2.5 nm, the longitudinal spacing is 3 nm, the cutting depth is 1 nm and the cutting speed is 200 m/s.

When the cutting distance is 12 nm, the cutting surface contour with lateral spacing x of 1, 1.5, 2 and 2.5 nm is shown in Fig.9a~9d. The wireframe line along the edge of the mesh surface is rendered in the figure. The cutting action of the abrasive leads to the extrusion deformation of the workpiece surface, which causes a large number of workpiece atoms to accumulate on the workpiece surface and the front end of the abrasive particles. With the increase of the lateral spacing between the two grinding grains, more and more atoms are deposited in front of the grinding grains, and in the cross region of the cutting trajectories of the two grinding grains. In order to quantitatively analyze the removal efficiency of workpiece atoms, statistics analysis on the number of removed atoms when the lateral spacing x is 1, 1.5, 2 and 2.5 nm is made, and the comparison result is shown in Fig.9e. As shown in Fig.9e, when the cutting distance is less than 3 nm, only one abrasive particle can cut into the workpiece, and the number of atoms removed is basically the same. When the cutting distance exceeds 3 nm, the second abrasive particle begins to touch the workpiece. The greater the lateral spacing, the more the removed atoms. This is because with the increase of lateral spacing, the number of atoms in contact with the abrasive particles increases, thus increasing the atomic removal ratio.

2.2.2 Effect of lateral spacing on cutting force change during micro cutting

In order to study the influence of lateral spacing on the cutting force of abrasive grains, the cutting forces in different directions produced by abrasive grains with different lateral spacing are compared and analyzed in this study. Fig.10 shows the comparison of cutting forces in different directions generated by the two abrasive particles when the lateral spacing x is 1, 1.5, 2 and 2.5 nm. It can be seen from Fig.10 that the lateral spacing has little influence on the cutting forces in all directions generated by the first grinding particle, while the cutting forces in each direction generated by the second abrasive particle increase with the increase of the lateral spacing of the abrasive particle. This is because the lateral spacing increases, the number of atoms in contact with the second abrasive particle increases, and the cutting force acting on the workpiece increases.

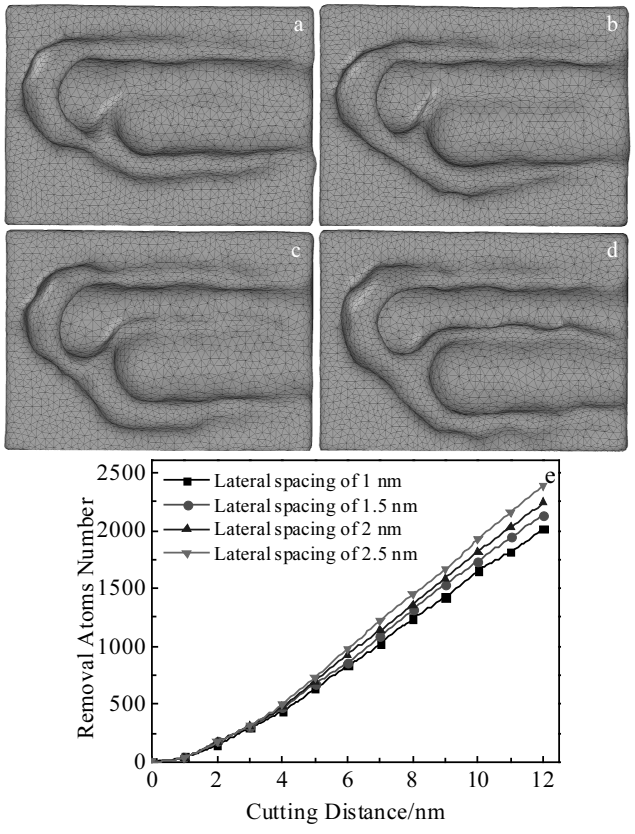

Fig.9 Cutting surface profiles at different lateral spacing (a~d) and curve of the number of removed atoms in workpiece (e): (a) x= 1 nm, (b) x=1.5 nm, (c) x=2 nm, and (d) x=2.5 nm

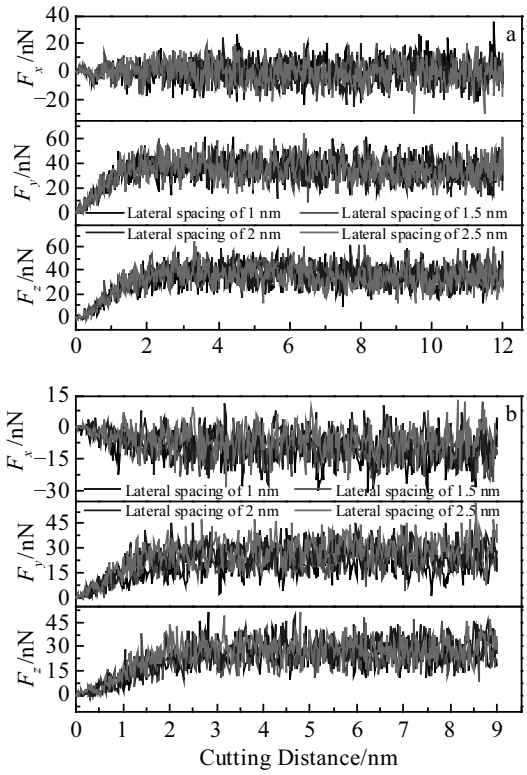

Fig.10 Cutting forces generated by the first (a) and the second (b) abrasive particles with different lateral spacing

2.2.3 Effect of lateral spacing on temperature and potential energy change during micro cutting

Different lateral spacing also has an impact on the temperature and potential energy of the workpiece. In order to study the influence of different lateral spacing on the temperature and potential energy change of the workpiece, a three-dimensional graph of temperature and potential energy change at different lateral spacing, as shown in Fig.11, is established. With the increase of the cutting distance, the temperature and potential energy in the cutting area of the Newton layer of the workpiece show an upward trend. When the cutting distance exceeds 6 nm, i.e., when the two abrasive particles cut into the workpiece completely, the upward trend slows down. With the increase of lateral spacing, the temperature and potential energy in the cutting area of Newton layer of workpiece rise faster, and the temperature and potential energy are higher when the cutting distance is 12 nm. The temperature is the highest when the lateral spacing is 2.5 nm, and the cutting distance is as high as 402 K when the cutting distance is 12 nm.

2.2.4 Effect of lateral spacing on lattice transformation and dislocation change during micro cutting

In order to study the effect of different lateral spacing on the lattice structure, Ackland-Jones analysis method was used to identify the crystal structure in the workpiece. The obtained crystal structure in the workpiece with different lateral spacing is shown in Fig.12. Fig.12a~12d show the lattice structure when the lateral spacing x=1, 1.5, 2 and 2.5 nm, respectively,

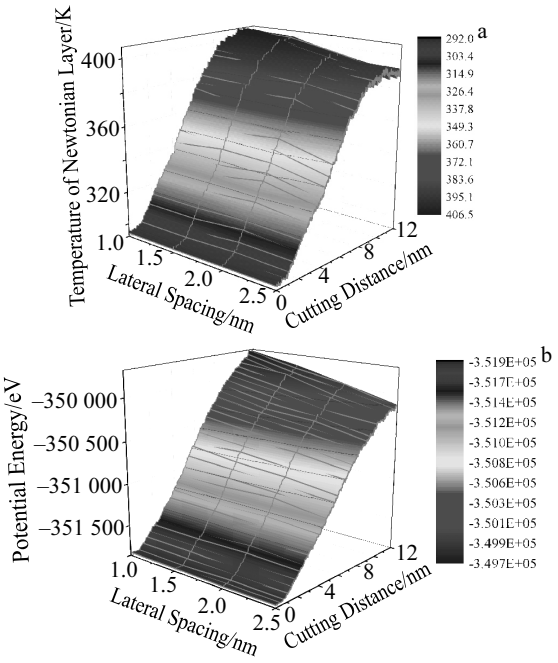

Fig.11 Three-dimensional curves of temperature (a) and potential energy (b) change

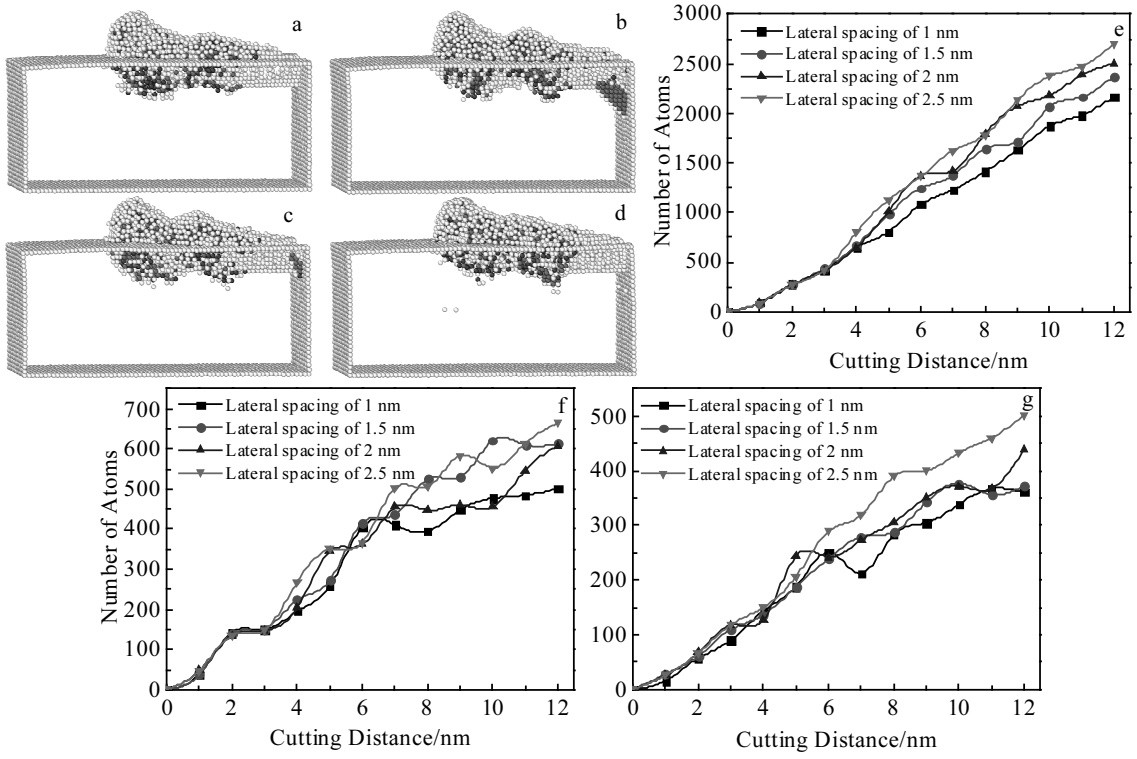

Fig.12 Lattice structure at different lateral spacing with cutting distance at 8 nm: (a) x=1 nm, (b) x=1.5 nm, (c) x=2 nm, and (d) x=2.5 nm; the number of atoms in different lattice structures: (e) dfcc structure, (f) hcp structure, and (g) bcc structure

with the cutting distance of 8 nm. According to the comparative analysis, dfcc structure, hcp structure, bcc structure and ico structure generate in the workpiece at different lateral spacing. With the increase of lateral spacing, the number and distribution of various lattice structures in the workpiece vary greatly due to the different energies required for the lattice to produce structural transformation. When x=1.5 nm and x=2 nm, there is a phenomenon of accumulation of hcp structure in the upper right corner of the workpiece, which is related to the formation, expansion and annihilation of dislocations and other defects. For quantitative analysis, the number of lattice structure atoms generated by transformation when the lateral spacing x is 1, 1.5, 2 and 2.5 nm is calculated and compared. Fig.12e~12g show the variation curves of dfcc, hcp, and bcc structure atoms, respectively. With the increase of lateral spacing, the number of various lattice structures in the workpiece changes significantly. The number of dfcc structures generated by transformation is the highest, while the number of bcc structures generated by transformation is the lowest. When the cutting distance is less than 3 nm, the number of atoms in various crystal structures increases with the extrusion and cutting effect of grinding particles on the workpiece, and the dislocation and other defects form and move, and the trend basically keeps unchanged. When the cutting distance exceeds 3 nm, with the increase of lateral spacing, the number of dfcc and bcc structure atoms generated by transformation increases, and the maximum number of converted atoms is 2698 and 502, respectively. However, for the hcp structure generated by transformation, it is less affected by the change of lateral spacing.

In order to study the dislocation evolution law of different lateral spacing, dislocation extraction algorithm was used to identify the dislocation defects in the workpiece. When the cutting distance is 8 nm, the effect of different lateral spacing on dislocation is shown in Fig.13.

Green, blue and yellow lines represent 1/6<112> Shocklley dislocation, 1/2<110> perfect dislocation and 1/3<100> Hirth dislocation, respectively. Dark blue represents the direction of Burgers vector of each dislocation. In Fig.13a, one Shocklley dislocation is 1.51 nm in length; in Fig.13b, there are two Shocklley dislocations and one Hirth dislocation, whose lengths are 2.48 and 2.29 nm, respectively; in Fig.13c, there are two Shocklley dislocations with length of 5.56 nm; in Fig.13d, there are 7 Shocklley dislocations and 2 perfect dislocations, the length of which is 13.19 and 1.686 nm. Dislocations occur in regions with complex atomic lattice structures. Under certain conditions, dislocations are interwoven in a certain form. The dislocation types generated by different lateral spacing are different. With the increase of lateral spacing, the number of dislocations generated in the workpiece increases gradually, and the total length of dislocations increases gradually.

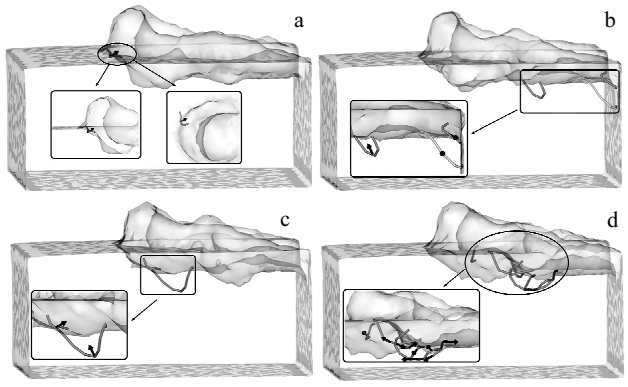

Fig.13 Effect of different lateral spacing on dislocation with cutting distance at 8 nm: (a) x=1 nm, (b) x=1.5 nm, (c) x=2 nm, and (d) x=2.5 nm

2.3 Effect of longitudinal spacing on cutting process

2.3.1 Effect of longitudinal spacing on material removal during micro cutting

In order to study the effect of the longitudinal spacing of the double abrasive grains on the micro cutting process, the longitudinal spacing is set as 2, 2.5 and 3 nm, the lateral spacing is 2.5 nm, the cutting depth is 1 nm and the cutting speed is 200 m/s.

When the cutting distance is 12 nm, the cutting surface contour with longitudinal spacing y of 2, 2.5 and 3 nm is shown in Fig.14a~14c, in which the wireframe line along the edge of the mesh surface is rendered. As shown in Fig.14, with the increase of the longitudinal spacing between the two grinding grains, the number of atoms stacked in front of the grinding grains becomes smaller and smaller, while the number of atoms stacked in the cross region of the cutting trajectories of the two grinding grains increases. In order to quantitatively analyze the removal efficiency of workpiece atoms, statistics analysis on the number of atoms removed when the longitudinal spacing y s 2, 2.5 and 3 nm is made. The comparison of the number of atoms removed with different longitudinal spacing is shown in Fig.14d. When the cutting distance is less than 2 nm, only one abrasive particle cuts the workpiece, and the number of atoms removed is basically the same. Although the surface area of the workpiece in contact with the second abrasive particle is the same, the number of removed atoms slightly decreases with the increase of longitudinal spacing. This phenomenon becomes more obvious with the increase of cutting distance when the cutting distance is more than 2 nm. This is because the smaller the longitudinal distance, the earlier the second grinding particle contacts the workpiece, and the more atoms removed by the first grinding particle are squeezed and stacked by the second grinding particle, the more atoms are removed.

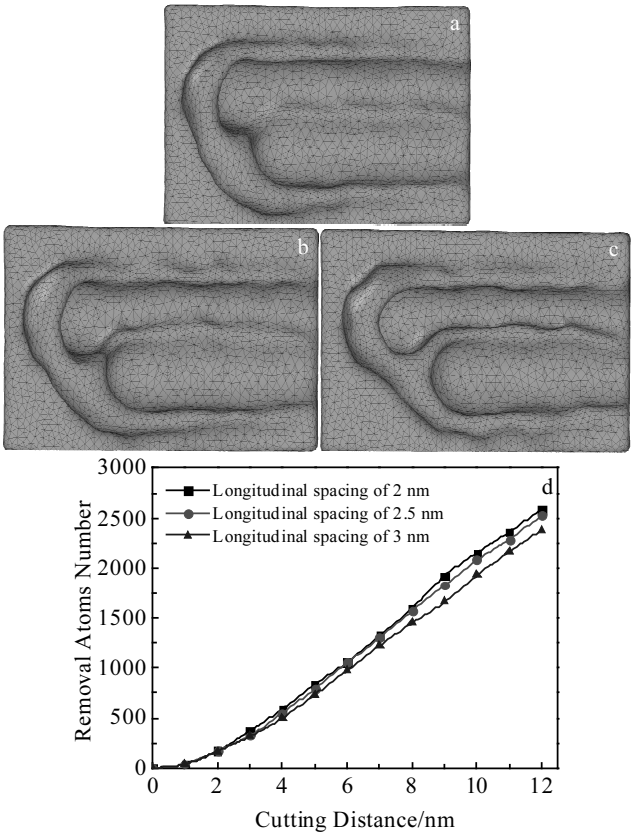

Fig.14 Cutting surface profiles at different longitudinal spacing (a~c) and curve of the number of removed atoms in workpiece (d): (a) y=2 nm, (b) y=2.5 nm, and (c) y=3 nm

2.3.2 Effect of longitudinal spacing on cutting force, temperature and potential energy change during micro cutting

In order to study the effect of longitudinal spacing on the cutting force of abrasive particles, this study made a comparative analysis of the cutting forces generated by abrasive particles with different longitudinal spacing in each direction. As shown in Fig.15, the cutting forces generated by two abrasive particles in each direction are compared under the condition of longitudinal spacing y is 2, 2.5 and 3 nm. Due to the different longitudinal spacing, the cutting distance of the second grinding particle is also different. The maximum cutting distance of 9 nm is selected for comparative analysis. As shown in Fig.15, with the increase of the longitudinal distance, the cutting force variation trend of the two grinding particles in each direction is basically the same, because of the same surface area of the workpiece in contact with the second grinding particle. The temperature and potential energy of the workpiece are also affected by different lateral spacing. As shown in Fig.16, with the increase of longitudinal spacing, the temperature and potential energy change trends of the cutting area of the Newton layer of the workpiece are basically the same.

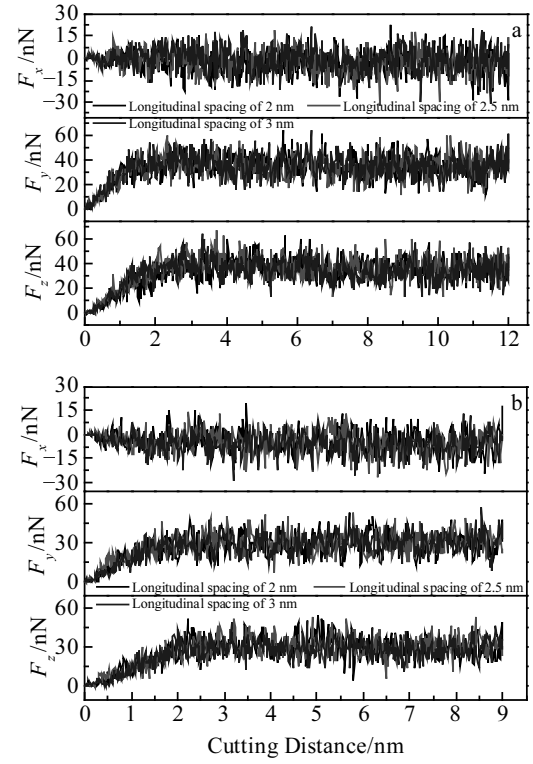

Fig.15 Cutting forces generated by the first (a) and the second (b) abrasive particles with different longitudinal spacing

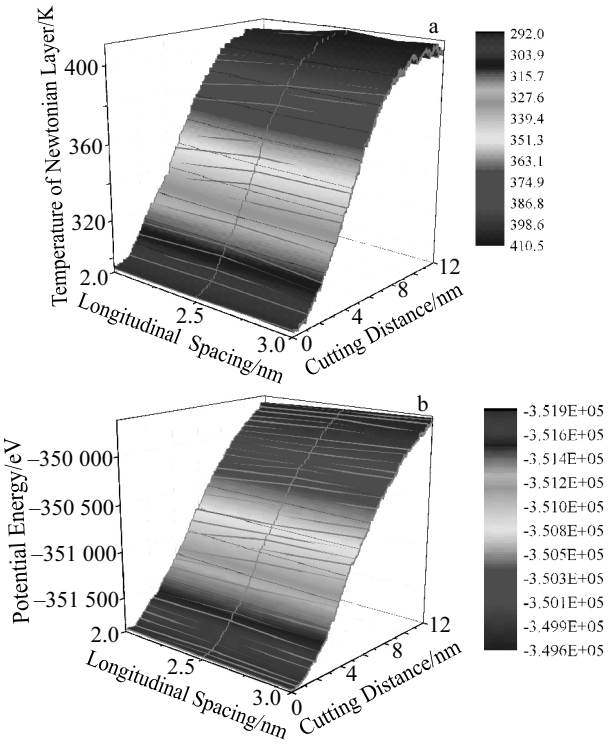

Fig.16 Three-dimensional curves of temperature (a) and potential energy (b) change at different longitudinal spacing

2.3.3 Effect of longitudinal spacing on lattice transformation and dislocation change during micro cutting

In order to study the effect of different longitudinal spacing on the workpiece lattice structure, the crystal structure in the workpiece was identified by the method of Ackland-Jones analysis. The lattice structure in the workpiece with different longitudinal spacing is shown in Fig.17. Fig.17a~17c show the lattice structure when the longitudinal spacing y=2, 2.5 and 3 nm, respectively, and the cutting distance is 8 nm. According to the comparative analysis, dfcc structure, hcp structure, bcc structure and ico structure are generated in the workpiece at different longitudinal spacing. With the increase of the longitudinal spacing, the number and distribution of all kinds of lattice structures in the workpiece are very different, but there is no phenomenon of accumulation of a large amount of structures. For quantitative analysis, the number of atoms transformed in lattice structures with different longitudinal spacing is calculated and compared in this study. Fig.17d~17f show the change curves of the number of atoms in dfcc, hcp and bcc structures, respectively. With the increase of the longitudinal spacing, the number of various lattice structures in the workpiece changes significantly, and the number of dfcc structures generated by transformation becomes less and less, while the number of hcp structures and bcc structures generated by phase transition is less correlated with the increase of longitudinal spacing. When the cutting distance is less than 2 nm, the number of atoms in various crystal structures increases, and the trend basically remains the same. When the cutting distance exceeds 2 nm, the smaller the longitudinal distance, the more the second abrasive particles contact the workpiece and the more various structures are generated. In the subsequent process, the fluctuation of the number of hcp structure and bcc structure may be caused by the formation, expansion and annihilation of dislocations and other defects.

In order to study the dislocation evolution law of different longitudinal spacing, dislocation extraction algorithm was used to identify the dislocation defects in the workpiece. When the cutting distance is 8 nm, the effect of different longitudinal spacing on dislocation is shown in Fig.18. In Fig.18, green, blue and red lines represent 1/6<112> Shocklley dislocation, 1/2<110> perfect dislocation and other dislocations, respectively. Dark blue arrow represents the direction of Burgers vector of each dislocation. In Fig.18a, there is a Shocklley dislocation with length of 3.48 nm. In Fig.18b, there are 3 Shocklley dislocations and 2 other dislocations, the length of which is 6.72 and 2.04 nm, respectively. In Fig.18c, there are 7 Shocklley dislocations and 2 perfect dislocations, the length of which is 13.19 and 1.686 nm, respectively. As shown in Fig.18, different types of dislocations are produced by different longitudinal spacing. With the increase of longitudinal spacing, the number of dislocations in the workpiece increases gradually, the total length of dislocations increases gradually, and the dislocation density also increases gradually.

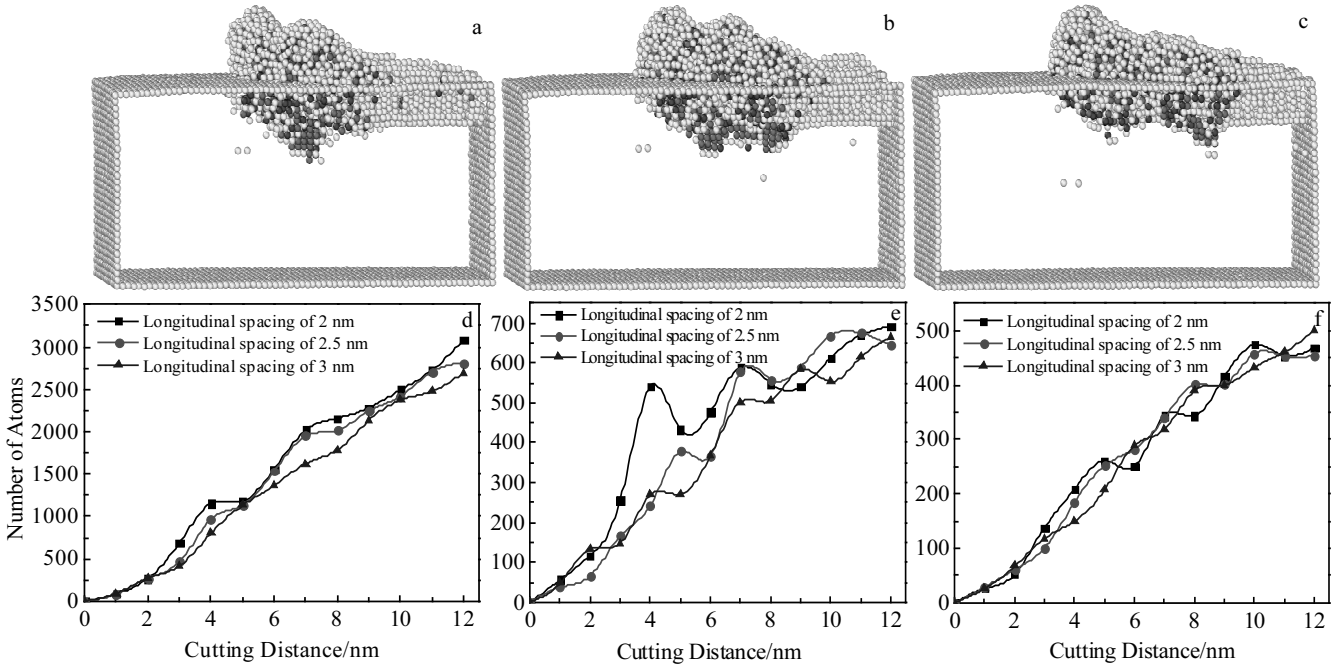

Fig.17 Lattice structures at different longitudinal spacing with cutting distance at 8 nm: (a) y=2 nm, (b) y=2.5 nm, and (c) y=3 nm; number of atoms in different structures: (d) dfcc structure, (e) hcp structure, and (f) bcc structure

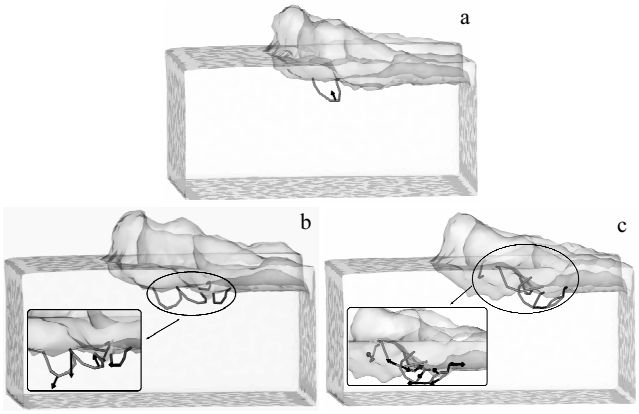

Fig.18 Effect of different longitudinal spacing on dislocation with cutting distance at 8 nm: (a) y=2 nm, (b) y=2.5 nm, and (c) y=3 nm

3 Conclusions

1) In the process of micro cutting single crystal γ-TiAl alloy with double abrasive particles, the workpiece of γ-TiAl alloy is subjected to the micro cutting effect of diamond abrasive particles, and the workpiece atoms generate displacement, removing from the surface of the workpiece in the form of chips, along with the movement of abrasive particles. The cutting process is accompanied by the generation of cutting heat, the change of potential energy and dislocation, and the lattice transformation.

2) The cutting force, cutting temperature, potential energy and removal efficiency increase with the increase of the lateral spacing, but are less affected by the longitudinal spacing. As the lateral and longitudinal spacing increases, the atoms in the cutting area migrate, the original lattice structure change, and the number, total length, and density of dislocations increase.

3) In the process of dual-abrasive micro cutting of γ-TiAl alloy workpiece, with the increase of lateral spacing, the number of dfcc and bcc structure atoms generated by the transformation of original fcc structure increases, while the number of hcp structure atoms is less affected by lateral spacing. With the increase of the longitudinal spacing, the number of dfcc structure atoms generated by the transformation of the original fcc structure decreases, while the number of hcp and bcc structure atoms is less affected by the longitudinal spacing.

References

1 Petare A C, Jain N K. *The International Journal of Advanced Manufacturing Technology*[J], 2018, 97(1-4): 741
2 Singh S, Kumar D, Sankar M R *et al*. *The International Journal of Advanced Manufacturing Technology*[J], 2019, 100(5-8): 1165
3 Petare A C, Jain N K. *Wear*[J], 2018, 404-405: 38
4 Zhang L,Yuan Z M, Qi Z J *et al*. *Powder Technology*[J], 2018, 333: 209
5 Li J Y, Meng W Q, Dong K *et al*. *Nanoscale Research Letters*[J], 2018, 13(1): 11
6 Lai M, Zhang X D, Fang F Z *et al*. *Precision Engineering*[J], 2017, 49: 160
7 Alhafez I A, Urbassek H M. *Computational Materials Science*[J], 2018, 143: 286
8 Zhu Z X, Gong Y D, Zhou Y G *et al*. *Science China Technological Sciences*[J], 2016, 59(6): 867
9 He L P, Zhu F L, Liu Y H *et al*. *AIP Advances*[J], 2017, 7(5): 561
10 Zhu Ying, Zhang Yincheng, Qi Shunhe *et al*. *Rare Metal Materials and Engineering*[J], 2016, 45(4): 897 (in Chinese)
11 Feng Ruicheng, Qiao Haiyang, Zhu Zongxiao *et al*. *Rare Metal Materials and Engineering*[J], 2019, 48(5): 1559 (in Chinese)
12 Li J H, Feng R C, Qiao H Y *et al*. *Metals*[J], 2019, 9(12): 1278
13 Li J Y, Meng W Q, Dong K *et al*. *International Journal of Precision Engineering and Manufacturing*[J], 2018, 19(11): 1597
14 Zhou P, Shi X D, Li J *et al*. *Ceramics International*[J], 2019, 45(12): 14 614
15 Daw M S, Baskes M I. *Physical Review B*[J], 1984, 29(12): 6443
16 Girifalco L A, Weizer V G. *Physical Review*[J], 1959, 114(3): 687
17 Ackland G J, Jones A P. *Physical Review B*[J], 2006, 73(5): 4104
18 Alexander S, Vasily V B, Athanasios A. *Modelling and Simulation in Materials Science and Engineering*[J], 2012, 20(8): 85 007

双磨粒微切削单晶 γ-TiAl 合金的材料去除机制

李俊烨，解鸿傀，张心明，赵伟宏，石广丰，徐成宇
(长春理工大学 跨尺度微纳制造技术教育部重点实验室，吉林 长春 130022)

摘　要：为了分析磨削过程中单晶 γ-TiAl 合金的材料去除机制，建立了双磨粒磨削 Ti-Al 合金的分子动力学模型。揭示了金刚石磨粒的横向间距和纵向间距对单晶 γ-TiAl 合金材料去除机制的影响。结果表明：单晶 γ-TiAl 合金的微切削过程中伴随有温度、势能、位错的变化以及晶格结构的转变；切削力、切削温度、势能以及去除效率随着横向间距的增加而增大，但受纵向间距的影响较小；晶格转变的原子数随横向间距的增加而增大，随纵向间距的增加而减小；随着横向间距和纵向间距的增加，位错数量、位错总长度以及位错密度相应增大。

关键词：单晶 γ-TiAl 合金；材料去除机制；分子动力学

作者简介：李俊烨，男，1981 年生，博士，教授，长春理工大学机电工程学院，吉林 长春 130022，E-mail: ljy@cust.edu.cn